Molecular Modeling Study of Leflunomide and Its Active Metabolite Analogues

Jarosław J. Panek,* Aneta Jezierska, Krzysztof Mierzwicki, Zdzisław Latajka, and Aleksander Koll

University of Wrocław, Faculty of Chemistry, 14 F. Joliot-Curie, 50-383 Wrocław, Poland

Received August 11, 2004

Leflunomide is known as a compound with various sorts of biological activity, which found a practical application in medicine. Search of current literature revealed an active metabolite of Leflunomide together with its eight analogues synthesized as protein tyrosine kinase inhibitors with potential anticancer activity. Accurate description of the molecular structure of these compounds is valuable. The detailed geometrical parameters description was performed using DFT theory. The conformational analysis and intramolecular proton transfer were considered. Using the most stable conformation the detailed electronic structure description was obtained by analysis of electron density and electrostatic potential distribution in the first step. Next, the topological analysis of the electron density by AIM method and electron localization function (ELF) theories supplemented this study. The AIM and ELF theories were applied to study the topology of the molecules, atomic charges distribution, and details of bonding. The theoretical investigations were performed in the gas phase and by using SCRF/PCM solvent reaction field. In this study the molecular modeling results for Leflunomide and the analogues of its active metabolite are presented.

1. INTRODUCTION

Molecular modeling techniques have grown during last 20 years to be powerful tools in drug research and discovery. The use of quantum chemistry not only provides us with great accuracy but also limits the size of systems that can be studied. In this respect, small molecules of potent biological activity are particularly well suited for this type of research. Leflunomide belongs to this class: it is a low-molecular-weight compound, has a relatively well studied metabolic path and mechanism of action, and its active metabolite together with its analogues are known. In recent years there appeared many publications discussing the diverse biological activity of Leflunomide. This compound was found to be a potent immunomodulator[1] acting as an inhibitor of tyrosine phosphorylation and pyrimidine nucleotide synthesis[2,3] which affects, among other processes, T-lymphocyte proliferation.[4] Its tyrosine kinase inhibiting activity permits Leflunomide to act also as an anticancer drug.[5] In addition it is being employed in the treatment of rheumatoid arthritis.[6] It was quickly found[7] that Leflunomide decomposed in vivo to form its active metabolite known as A77 1726. This metabolite served as an initial point in synthesis of modified analogues with potential anticancer activity.[8,9] Attempts to employ molecular modeling to Leflunomide and its metabolite are restricted to docking studies[10,11] and pharmacophore identification.[12] Another study[13] is based on semiempirical methods. The references cited so far are only a very small part of the vast research reported in the literature on Leflunomide and related compounds. The main goal of the study presented below is the detailed molecular structure and the electronic structure description of the above mentioned compounds using molecular modeling and advanced quantum chemistry techniques. The structures of investigated compounds are presented in Figure 1. The theoretical study is divided into two parts. The detailed description of geometrical parameters was obtained as a result of conformational analysis. The solvent influence on the geometrical structure was also studied. Next, the intramolecular hydrogen bond was investigated for analogues of A77 1726. The steric

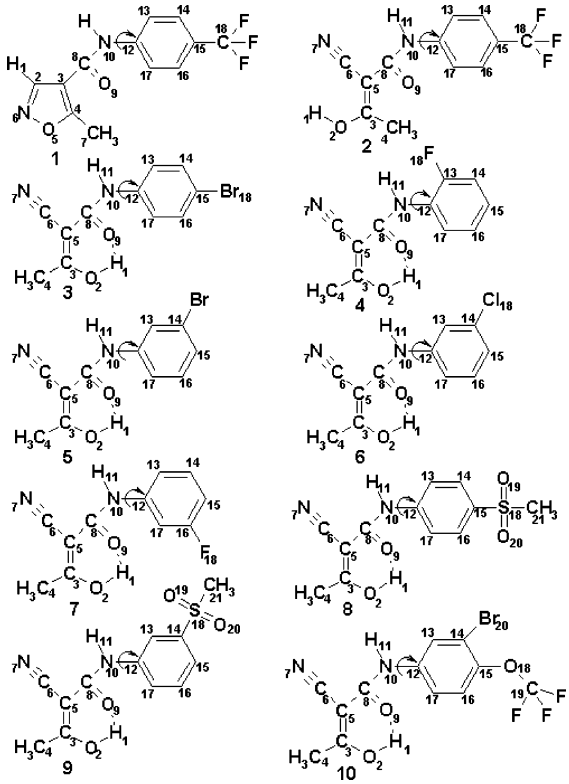

Figure 1. The structures of Leflunomide (**1**), its active metabolite (**2**), and metabolite analogues (**3**−**10**). The atom numbering scheme given here is used throughout the paper, especially for AIM and ELF results. The arrows show the dihedral angles taken into account during conformational analysis.

* Corresponding author phone: +48 71 3757246; fax: +48 71 3282348; e-mail: jarek@elrond.chem.uni.wroc.pl.

10.1021/ci049754d CCC: $30.25
Published on Web 12/09/2004

and induction effects were taken into consideration, and the forms with and without intramolecular hydrogen bond were studied. In the next step the detailed electronic structure description was performed finding parts of the molecules responsible for the reactivity and the most sensitive for internal interactions. This part of the study contains calculations in the gas phase and with the solvent reaction field reproduced by application of polarizable continuum model (SCRF/PCM). The calculations consist of a few steps. First, the electron density and electrostatic potential were analyzed. Next, the Atoms in Molecules (AIM) theory found an application to characterize the topology of the electron density and to generate atomic charges in both gas-phase and polar environments for studied molecules. To enrich the electronic structure investigations the electron localization function (ELF) was applied to study differences in the bonding of the analyzed molecules. The theoretical description of Leflunomide, its active metabolite, and the metabolite analogues performed along lines described above will be very useful in the understanding of molecular scale processes occurring in the presence of these compounds. The outline of the article is as follows: in section 2 the details of computational methodology are presented, the obtained results are discussed in section 3, while concluding remarks are in section 4.

2. MOLECULAR MODELING METHODOLOGY

The theoretical description of the analyzed compounds consists of several parts. The geometry optimization in the gas phase was performed using the Gaussian 03 suite of programs[14] at the B3LYP/6-311+G(d,p) level.[15−18] The B3LYP DFT functional[15,16] is known for a relatively good performance and a moderate computational cost. Harmonic vibrational analysis was performed confirming that the obtained structures were not transition states. Conformational relaxed scans were performed with dihedral angle increment of 15° (24 steps). Figure 1 indicates the angles taken into account during the procedure. Details of the proton position in the hydrogen bridge were investigated with adiabatic, rigid scans involving movement of the proton engaged in the intramolecular hydrogen bond. The proton was displaced along a circular arc defined by equilibrium positions of the donor, hydrogen, and acceptor atoms. Details of this procedure are described elsewhere.[19] For the most stable conformers, electron density and electrostatic potential maps were generated both in the gas phase and with the dielectric polarizable continuum model[20] SCRF/PCM, which simulates the effects of a polar environment (water as a solvent, ϵ=78.39) on the molecular properties of investigated compounds. Differential maps of these properties (solvent vs gas phase) were used to indicate the most reactive parts of the molecules. The mapping of the electrostatic potential is an established technique for investigation of biologically active compounds[21] and constitutes a vital element of a 3D-QSAR CoMFA approach.[22] A detailed description of the electronic structure was performed according to the Atoms in Molecules (AIM) theory of R. F. W. Bader.[23,24] The theory was used for two purposes: generation of atomic charges in the gas phase and within the SCRF/PCM solvent reaction field and topological characterization of electron density distribution. This part of the study was performed using the original AIMPAC package of Bader and co-workers.[25] To enrich the study of geometry of the biologically active compounds, additional geometry optimizations for compounds **1**, **2**, and **8** were performed using the SCRF/PCM solvent model.[20] The main purpose of these calculations was the study of solvent influence on the geometry of the studied compounds. The last part of the calculations was also connected with the electronic structure description. The theory proposed by Silvi and Savin[26] was used for the partitioning of space according to the Electron Localization Function (ELF). This partitioning was performed with TopMod package of Silvi and co-workers.[27] Various parts of visualization were rendered using gOpenMol[28] and Molekel[29] programs without taking bond order into account, i.e., single, double, and triple bonds are presented in the same way. Contour maps of the electron density topology were prepared with the AIMPAC package, which produces drawings of density contours and bond paths in a selected plane. Therefore, some parts of the molecules deviating from the plane are not shown in detail.

The AIM and ELF topological methods are much less popular than the classical schemes for electronic structure analysis. AIM, initiated by R. F. W. Bader, is an effort to provide chemists with unique definitions of such concepts such as an atom, bond, or functional group based solely on the properties of electron density and its gradient field. In our paper the AIM theory was used for two purposes. First, the chemical bonding topology was investigated by the drawing of bond paths and the analysis of bond and ring critical points, with special attention paid to the intramolecular hydrogen bond. The presence of this bond was confirmed theoretically by the AIM method according to the criteria of Popelier.[30] Second, integration of electron density over atomic basins yielded atomic charges, which are generally thought to be less dependent on the level of calculations than other population analysis schemes.[31] The partitioning of molecular space by the ELF method provides information of another kind: the space is divided into basins of different bonding functionality. There are core basins, related to chemically inert electron density, and valence basins (bonds and lone pairs). Analysis of the population of these basins defined variations in the bonding electron density distribution under influence of substituents and polar environment modeled using the SCRF/PCM method.

3. RESULTS AND DISCUSSION

Geometrical Parameters. The study of geometrical parameters is necessary for the proper understanding of flexibility and related molecular properties, especially for bioactive compounds. The analyzed database consisted of 10 compounds, which are as follows: Leflunomide (**1**), its active metabolite (**2**), and eight analogues (**3**−**10**) of the metabolite (see Figure 1). The analogues and metabolite are similar in conformational properties in distinction from Leflunomide, which contains the isoxazole ring. The process of ring opening leads to the formation of a new bonding structure resulting in the appearance of new functional groups. The eight analogues are the results of synthesis as opposed to the active metabolite, which is formed in the biochemical process. The detailed theoretical description of these compounds is presented below in an effort to underline the differences in structure and bonding.

The electronic structure description in the next chapter is based partially on differential maps of studied properties.

Table 1. Structural Parameters of Leflunomide (**1**) at B3LYP/6-311+G(d,p) Level

geometrical parameters	gas phase	SCRF/PCM
Bond Lengths [Å]		
H(1)−C(2)	1.0819	1.0814
C(2)−C(3)	1.4299	1.4274
C(3)−C(4)	1.3754	1.3746
C(4)−O(5)	1.3405	1.3421
O(5)−N(6)	1.4029	1.4098
N(6)−C(2)	1.3028	1.3039
C(4)−C(7)	1.4841	1.4827
C(3)−C(8)	1.4804	1.4792
C(8)−O(9)	1.2211	1.2279
C(8)−N(10)	1.3822	1.3741
N(10)−H(11)	1.0084	1.0102
N(10)−C(12)	1.4071	1.4054
C(12)−C(13)	1.4048	1.4054
C(13)−C(14)	1.3846	1.3848
C(14)−C(15)	1.3971	1.3987
C(15)−C(16)	1.3925	1.3936
C(16)−C(17)	1.3919	1.3917
C(12)−C(17)	1.4007	1.4018
C(15)−C(18)	1.5012	1.4969
Valence Angles [deg]		
C(2)−C(3)-C(4)	103.23	103.78
C(3)−C(4)-O(5)	109.16	109.01
C(4)−O(5)-N(6)	110.11	109.87
O(5)−N(6)-C(2)	104.92	105.07
C(3)−C(4)-C(7)	134.00	134.11
C(2)−C(3)-C(8)	130.97	130.03
C(3)−C(8)-O(9)	122.27	121.90
C(8)−N(10)-C(12)	128.96	129.11
N(10)−C(12)-C(13)	117.00	116.86
Dihedral Angles [deg]		
C(2)−C(3)-C(4)−C(7)	179.50	179.90
C(2)−C(3)-C(4)−O(5)	−0.30	−0.43
C(3)−C(4)-O(5)−N(6)	0.42	0.61
C(4)−O(5)-N(6)−C(2)	−0.35	−0.52
C(3)−C(8)-N(10)−C(12)	−178.71	−175.75
O(9)−C(8)-N(10)−C(12)	1.46	4.05
C(8)−N(10)-C(12)−C(13)	−178.27	−174.83

This requires usage of identical structures for showing the most sensitive places of the molecules, because differential maps are heavily influenced by even small changes in the geometry due to high electron density values near the nuclei. To verify the solvent influence on the molecular geometry, optimizations were performed both in the gas phase and using the SCRF/PCM solvation model. The results obtained at the B3LYP/6-311+G(d,p) level are presented in Tables 1 and 2 for Leflunomide (**1**), the active metabolite and one of its analogues (**2**, **8**), respectively. The differences between the gas phase and the solvent model are rather small and restricted to atoms with lone electron pairs (O5 and N6 of the isoxazole ring, C8−O9 and C8−N10 of the amide group in Leflunomide **1**). In the case of the active metabolite **2** the elongation of the C3−C5 double bond and the O2−C3 bond is observed in the solvent. The analogue **8** has an intramolecular hydrogen bond which prevents the O2−C3 distance from changing, but both **2** and **8** exhibit changes in the amide group (C8−O9 and C8−N10). N10−H11 changes very slightly. What is however most important, the overall conformation of the molecules is almost unaffected by the solvent, as witnessed by the values of dihedral angles.

As a first step of the geometrical structure modeling, a conformational search was performed. The results for the dihedral angle defining the mutual position of the aromatic ring and the amide bond (C8−N10−C12−C13, see Figure 1) of four selected compounds are presented in Figure 2. The rest of the molecule is held in a rather rigid conformation by both the C3−C5 double bond and the O2−H1···O9 intramolecular hydrogen bond. According to our gas-phase molecular modeling, the molecules prefer a planar arrangement of the phenyl ring and the amide bond, stabilized by resonance coupling between these moieties. Both the shape (minima at 0° and 180°) and barrier height (4−5 kcal/mol) are practically the same for all the compounds. The notable exception is observed for **4**, which is ortho-substituted with fluorine (see Figure 2, lower left diagram). The fluorine atom, being strongly electronegative, gathers much of the negative charge. The dihedral angle of 180° would mean that this atom and the O9 oxygen atom of the carbonyl group would be located in close proximity. This causes not only a steric hindrance (**4** is the only ortho-substituted compound in the series) but also a strong electrostatic repulsion. Therefore, for **4** this dihedral angle value signifies a maximum on the potential energy curve. Another unexpected feature of the conformational profiles is a slight asymmetry of the maxima for **8** (Figure 2, lower right diagram) resulting from the fact that the potential energy scans were relaxed, i.e., with full optimization with respect to other remaining degrees of freedom. The optimized structure of **8** is almost planar, but nevertheless of C_1 symmetry, and this enabled the sulfonyl group to rotate slightly during the barrier crossing, and subsequently the corresponding maxima were not equivalent.

Leflunomide and its active metabolite do not possess an intramolecular hydrogen bond. This interaction is however present in the eight analogues, which were described by Xu et al.,[3,5] and it is responsible for their 3D molecular arrangement. It has a stabilizing effect on the conformation shown in Figure 1. Our theoretical investigations are aimed at an estimation of the strength of this bond and the possibility of the coexistence of two molecular forms: with and without the hydrogen bond. As a model compound, the analogue **8** was used, and the result of the conformational scan for the O−H donor group is presented in Figure 3. The hydrogen-bonded form is energetically preferable, while the open form is 19 kcal/mol less stable. The barrier from open to closed form is only 3.9 kcal/mol, and for the reverse direction it is 22.9 kcal/mol. The conformation with the intramolecular hydrogen bond is thus preferred, and the bond itself is rather strong. Therefore the next step of our study is the investigation of proton dynamics in the bridge. The potential energy curve was obtained by moving the proton along the arc from the donor to acceptor atoms while keeping other nuclei fixed, as described in the Molecular Modeling section. A graphical representation of the results is presented in Figure 4. The molecular form is preferred over the proton-transferred form, which however is also a minimum on the potential energy curve. The investigations were performed in both gas-phase and polar environments, and the latter enhances the possibility of finding the proton near the acceptor: the barrier is lowered from 13 to 11 kcal/mol. The secondary minimum is 12 kcal/mol less stable than the molecular form in the gas phase, and the difference drops to 10 kcal/mol in the polar environment. Such potentials were determined for all the compounds **3**−**10,** and it turned out that they practically did not depend on the substituent in the aromatic ring.

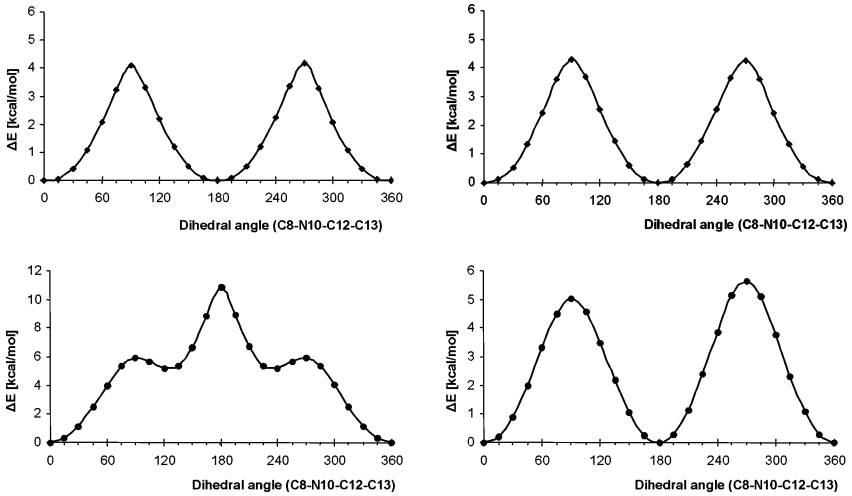

Figure 2. Conformational analysis results for compound **1** (upper left), **2** (upper right), **4** (lower left), and **8** (lower right). The energy changes are relative to the global minimum conformation.

Table 2. Structural Parameters of the Active Metabolite of Leflunomide (**2**) and One of Its Analogues (**8**) at B3LYP/6-311+G(d,p) Level

	2		**8**	
geometrical parameters	gas phase	SCRF/ PCM	gas phase	SCRF/ PCM
	Bond Lengths [Å]			
H(1)−O(2)	0.9644	0.9678	1.0046	1.0053
O(2)−C(3)	1.3475	1.3381	1.3152	1.3158
C(3)−C(4)	1.4928	1.4889	1.4918	1.4888
C(3)−C(5)	1.3663	1.3752	1.3841	1.3875
C(5)−C(6)	1.4257	1.4212	1.4179	1.4148
C(6)−N(7)	1.1575	1.1586	1.1588	1.1594
C(5)−C(8)	1.5025	1.4946	1.4775	1.4765
C(8)−O(9)	1.2226	1.2272	1.2426	1.2461
C(8)−N(10)	1.3760	1.3754	1.3654	1.3626
N(10)−H(11)	1.0115	1.0115	1.0122	1.0121
N(10)−C(12)	1.4067	1.4048	1.4085	1.4059
C(12)−C(13)	1.4044	1.4055	1.4043	1.4051
C(13)−C(14)	1.3854	1.3852	1.3862	1.3855
C(14)−C(15)	1.3964	1.3979	1.3938	1.3953
C(15)−C(16)	1.3934	1.3942	1.3918	1.3928
C(16)−C(17)	1.3909	1.3912	1.3913	1.3908
C(17)−C(12)	1.4015	1.4026	1.4021	1.4032
C(15)−C(18)	1.5008	1.4963	1.8012	1.7932
	Valence Angles [deg]			
O(2)−C(3)-C(4)	115.95	116.29	114.04	114.15
C(4)−C(3)-C(5)	127.62	127.61	124.25	124.58
O(2)−C(3)-C(5)	116.43	116.10	121.71	121.27
C(3)−C(5)-C(6)	118.06	117.10	120.93	119.92
C(3)−C(5)-C(8)	123.86	124.17	119.71	119.99
C(6)−C(5)-C(8)	118.08	118.73	119.36	120.09
C(5)−C(8)-O(9)	123.26	123.06	120.62	120.25
C(8)−N(10)-C(12)	128.78	128.91	129.45	129.41
O(9)−C(8)-N(10)	123.13	122.73	122.98	122.71
N(10)−C(12)-C(13)	116.70	116.71	116.48	116.40
	Dihedral Angles [deg]			
O(2)−C(3)-C(5)−C(6)	−0.01	1.43	−179.89	−179.95
O(2)−C(3)-C(5)−C(8)	−179.99	−178.07	0.09	0.06
C(6)−C(5)-C(8)−O(9)	179.89	−169.60	179.77	179.82
C(5)−C(8)-N(10)−C(12)	−179.94	−178.32	−179.79	179.90
O(9)−C(8)-N(10)−C(12)	0.06	1.30	0.22	−0.03
C(8)−N(10)-C(12)−C(13)	179.66	−177.15	−178.85	−178.53

Electronic Structure. The second part of the Results and Discussion section contains the electronic structure description for investigated molecules. The outline of this part is as follows: first, the electron density and electrostatic potential distribution is analyzed using isosurface maps. Next, the advanced AIM theory is used to show the bonding and atomic charges distribution. The last part contains a discussion of electron localization function results.

Differential maps of electron density and electrostatic potential were prepared for Leflunomide (**1**), its active metabolite (**2**), and model analogue (**8**). The maps for other analogues are very similar, so the graphical presentation was

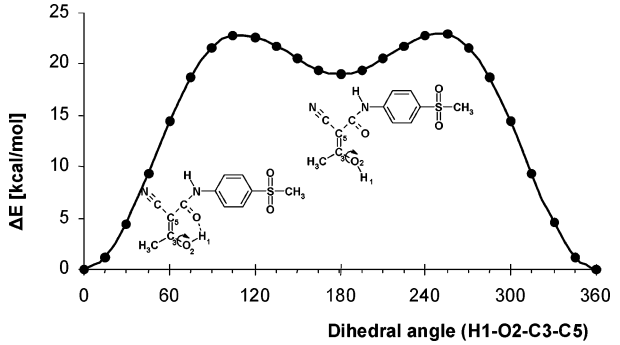

Figure 3. Conformational analysis of intramolecular hydrogen bond for compound **8**. The energy changes are relative to the global minimum conformation.

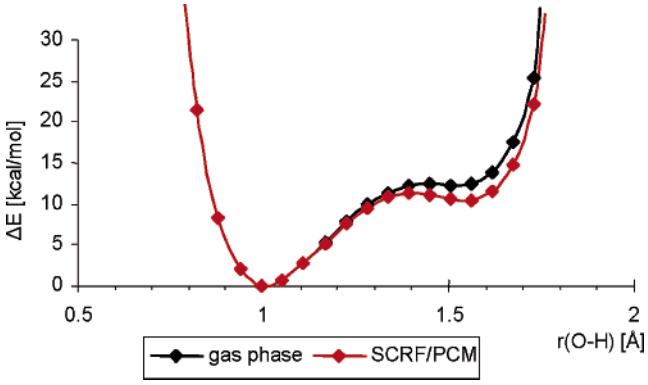

Figure 4. Potential energy function of proton movement in the O2−H1···O9 intramolecular hydrogen bond of molecule **8**. The energy changes are relative to the global minimum conformation.

made only for the three compounds named above, chosen as the most differing in the database of compounds **1**−**10**. The maps were obtained by subtracting the gas-phase values from the ones computed using the SCRF/PCM solvent model at the same, gas-phase-optimized geometry. This method is useful for detection of electron density and electrostatic potential redistribution under environmental influence. Figure 5 presents differential maps of electron density. In the case of Leflunomide (**1**), the largest variations are seen on the heteroatomic edge of the isoxazole ring and on the H11 atom of the amide bond. The most significant, however, is the variation on the H1 atom connected with the isoxazole ring. This atom is thought to be responsible for the process of ring opening.[7] For an active metabolite (**2**) the most significant changes occur in the C≡N group and terminal H1 atom. In the case of compound **8**, also the C≡N group is very strongly polarized by the solvent, but the H1 hydrogen atom is engaged in the intramolecular hydrogen bond and the environment has no visible effect upon it. Instead, electron density changes are present in the SO_2CH_3 substituent of the phenyl ring, which has many electron lone pairs. Electrostatic potential (ESP) is also a property closely derived from electron density. Moreover, ESP is very important for bioactive compounds, because it plays a key role in the initial steps of ligand−receptor interactions. The ESP differential maps for compounds **1**, **2**, and **8** are presented in Figure 6. The procedure of map generation is the same as described above. Leflunomide gathers more negative ESP around the edge of the isoxazole ring and the carbonyl group of the amide bond, but there is a wide region of more positive ESP values around the proton-rich edge

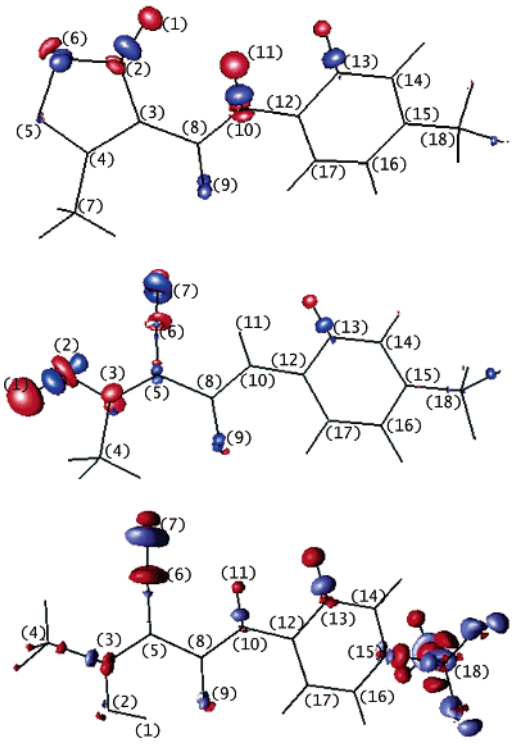

Figure 5. Differential map of the electron density for compounds (top to bottom) **1**, **2**, and **8**: red color marks regions of decrease (−0.004 au for **1**, −0.003 au for **2**, and −0.002 au for **8**), while blue − of increase (0.004 au for **1**, 0.003 au for **2**, and 0.002 au for **8**) in electron density upon SCRF/PCM treatment with dielectric permittivity of water (ϵ=78.39).

defined by atoms H1, H11 of the amide bond and C13 of the phenyl ring. After the isoxazole ring opening, there appear new functional groups in the active metabolite molecule (**2**) and different electrostatic potential distribution. The most visible is a region of lowered ESP around the C≡N group, present in both compounds **2** and **8**. The unbound O−H group of **2** is an area of significant increase in ESP. At this place occurrence of an intermolecular hydrogen bond is very probable. In the case of **8**, this group is involved in an intramolecular hydrogen bond, and the differences in ESP are not visible upon SCRF/PCM treatment. On the other hand, there is a region of increased ESP near H11 and C13 atoms, similar to that of Leflunomide. The mentioned above lone pairs of oxygen atoms of the sulfonyl group are responsible for a large domain of decrease in ESP in **8**. The differential maps have thus shown qualitative differences between studied molecules at a molecular level.

The AIM contour maps of electron density topology are presented in Figure 7. The bond paths (in red) intersect contours of electron density. The saddle points of the bond paths are named bond critical points (BCPs), and the point located in the middle of a ring is a ring critical point (RCP). The presence of BCPs and respective bond paths is theoretical proof for the bonding network in the molecule. Particularly, the presence of a hydrogen bond in the molecule **8** is indicated by its bond path (marked as green line). The values of electron density and its Laplacian at the hydrogen bond BCP are listed in Table 3 for all the analogues **3**−**10**. These values are consistent with the Popelier criteria for hydrogen bond presence[30] and indicate a case of a strong hydrogen bond. As seen in Table 3, the influence of a polar environment is not strong, but a slight weakening of hydrogen bond

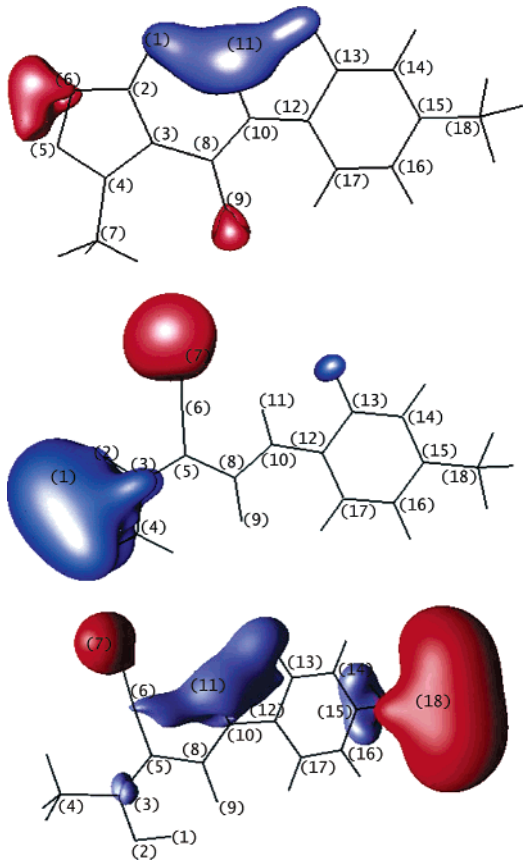

Figure 6. Differential map of the electrostatic potential for compounds (top to bottom) **1**, **2**, and **8**: red color marks regions of decrease (−0.016 au for **1**, −0.014 au for **2** and **8**), while blue − of increase (0.03 au for **1**, 0.014 au for **2** and **8**) in electrostatic potential upon SCRF/PCM treatment with dielectric permittivity of water (ϵ=78.39).

Table 3. Electron Density and Its Laplacian at the Hydrogen Bond Critical Point of Compounds **3**−**10**

ρ [e/bohr^3]	gas phase	SCRF/PCM
3	0.0620	0.0618
4	0.0626	0.0624
5	0.0620	0.0618
6	0.0622	0.0619
7	0.0617	0.0615
8	0.0605	0.0602
9	0.0611	0.0608
10	0.0607	0.0605
$\nabla^2\rho$ [e/bohr^5]	gas phase	SCRF/PCM
3	0.1532	0.1538
4	0.1542	0.1548
5	0.1534	0.1540
6	0.1535	0.1541
7	0.1531	0.1538
8	0.1525	0.1530
9	0.1531	0.1534
10	0.1527	0.1532

is observed. There is no clear relation between the phenyl ring substituent type and the parameters of hydrogen bond BCP.

To complete the electronic structure description based on the AIM theory, the atomic charges of atoms from a common substructure of **1**−**10** computed within this approach are presented in Tables 4−6. Because of a different atom numbering scheme for Leflunomide (**1**) and other molecules, the data for **1** are grouped in a separate Table 4. In case of

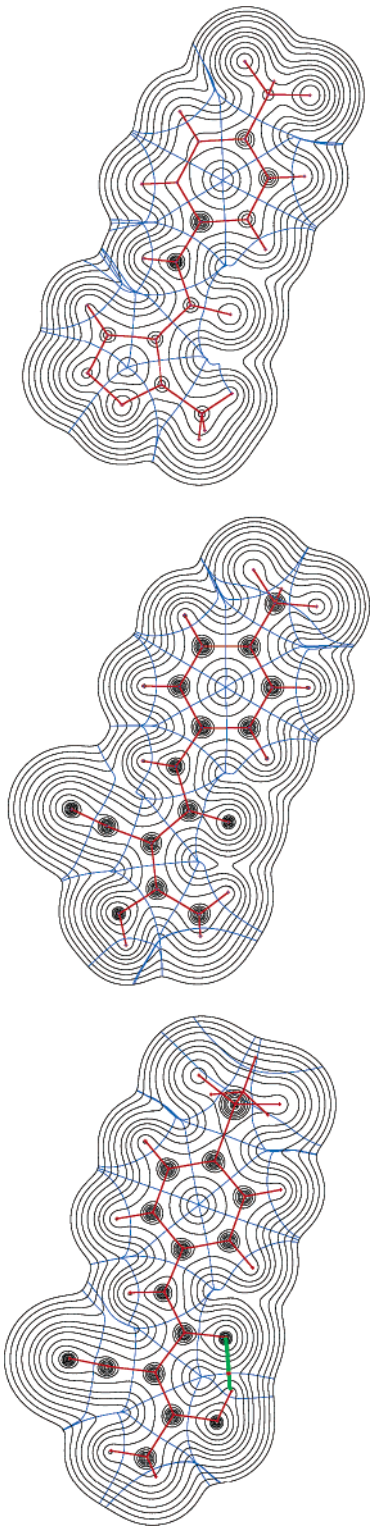

Figure 7. Cross-sections through the electron density calculated in the gas phase at the DFT B3LYP/6-311+G(d,p) level. Red lines − AIM bond paths, blue lines − interatomic boundaries according to the definition of Bader, green line and red dot − bond path and critical point of the intramolecular hydrogen bond. Top: compound **1** (Leflunomide), middle: **2** (active metabolite), bottom: **8**.

this molecule, the most significant changes occur at the H1, O5, N6, O9, and H11 atoms. These atoms are exposed, because they belong either to the edge of the isoxazole ring (H1, O5, N6) or to the amide bond (O9, H11). The fact that they are both exposed and strongly polarizable makes them good targets for external interactions. These interactions can

Table 4. AIM Partial Atomic Charges for Leflunomide (**1**)

	gas phase	SCRF/PCM
H(1)	0.0609	0.1236
C(2)	0.5276	0.5292
C(3)	−0.0290	−0.0183
C(4)	0.5107	0.5088
O(5)	−0.7118	−0.7327
N(6)	−0.5056	−0.5647
C(7)	0.0401	0.0369
C(8)	1.3882	1.3885
O(9)	−1.1280	−1.1680
N(10)	−1.1255	−1.1307
H(11)	0.3788	0.4372
C(12)	0.3566	0.3538
C(13)	−0.0066	−0.0125
C(14)	0.0144	−0.0019
C(15)	0.0247	0.0113
C(16)	0.0098	−0.0040
C(17)	0.0080	−0.0066

be of a different nature, because groups C2−H1 and N10−H11 are potential hydrogen bond donors, while the remaining atoms are equipped with lone pairs and can act as acceptors of hydrogen bonds. This leads us directly to molecule **2**, which is formed when the isoxazole ring of Leflunomide opens at atom H1. Further, atomic charges for discussed open molecules **2**−**10** are presented in Tables 5 and 6. The charge of H1 atom is markedly different between **2** (+0.58 e) and other analogues (+0.64 e) in the gas phase. The cause is an intramolecular hydrogen bond present in **3**−**10**. An increase of net charge of the hydrogen atom is also one of Popelier's criteria for hydrogen bond. The situation is, however, different in the solvent reaction field (Table 6), where H1 net charge is almost constant for **2**−**10**; the same can be said about the O2 atomic charge. This is another manifestation of a hydrogen bond shielding atoms H1 and O2 from external interactions for compounds **3**−**10**. Thus, comparing gas and solvent models, a sharp increase in the charge of H1 atom is observed only for **2**, in which this atom is not engaged in the intramolecular hydrogen bond. This increase shows that the polar solvent acts on the H1 and O2 atoms of **2** in a way similar to the action of the intramolecular hydrogen bond for **3**−**10**, and this is the reason for the mentioned similarity of the atomic charges within SCRF/PCM model. The influence of polar solvent is visible mostly in the case of atoms N7, O9, and H11, which is consistent with differential maps described above.

In the last part of this section, the ELF results are discussed. Figure 8 represents ELF = 0.85 isosurface for compounds **1**, **2**, and **8**. The figure shows clearly the most important features of the ELF description of molecular properties. Very small core domains, located around nuclei, are linked by bonding regions (*disynaptic valence domains*). Lone pairs are described as larger *monosynaptic domains*, which in the case of halogen and some oxygen atoms have a distinct toroid shape. The electronic populations of selected basins are given in Tables 7 (Leflunomide), 8, and 9.

Table 5. AIM Partial Atomic Charges for Compounds **2**−**10** Computed in the Gas Phase

	2	**3**	**4**	**5**	**6**	**7**	**8**	**9**	**10**
H(1)	0.5815	0.6370	0.6372	0.6380	0.6388	0.6384	0.6375	0.6387	0.6381
O(2)	−1.0737	−1.1285	−1.1292	−1.1285	−1.1286	−1.1284	−1.1267	−1.1277	−1.1270
C(3)	0.5680	0.6670	0.6662	0.6674	0.6659	0.6626	0.6691	0.6657	0.6671
C(4)	−0.0004	0.0233	0.0232	0.0227	0.0236	0.0252	0.0228	0.0241	0.0244
C(5)	0.0665	0.0319	0.0332	0.0333	0.0343	0.0343	0.0331	0.0353	0.0350
C(6)	0.8092	0.8192	0.8195	0.8183	0.8191	0.8163	0.8200	0.8195	0.8184
N(7)	−1.0975	−1.1258	−1.1188	−1.1241	−1.1241	−1.1258	−1.1219	−1.1196	−1.1216
C(8)	1.3946	1.3542	1.3508	1.3487	1.3505	1.3557	1.3522	1.3479	1.3517
O(9)	−1.1374	−1.1417	−1.1422	−1.1412	−1.1412	−1.1406	−1.1394	−1.1415	−1.1405
N(10)	−1.1377	−1.1504	−1.1540	−1.1481	−1.1481	−1.1505	−1.1488	−1.1478	−1.1475
H(11)	0.4055	0.4068	0.4317	0.4076	0.4076	0.4078	0.4090	0.4107	0.4097
C(12)	0.3599	0.3480	0.3752	0.3528	0.3534	0.3528	0.3569	0.3564	0.3612
C(13)	−0.0030	−0.0022	0.4476	0.0214	0.0198	−0.0078	0.0003	0.0051	0.0290
C(14)	0.0127	0.0286	0.0190	−0.0829	0.0544	0.0081	0.0151	0.0058	−0.0577
C(15)	0.0247	−0.0964	−0.0009	0.0173	0.0170	0.0091	−0.1613	0.0035	0.4545
C(16)	0.0096	0.0263	−0.0026	0.0024	0.0038	0.4683	0.0124	−0.1483	0.0247
C(17)	0.0067	0.0080	0.0062	0.0037	0.0026	0.0244	0.0101	0.0057	0.0148

Table 6. AIM Partial Atomic Charges for Compounds **2**−**10** Computed within the SCRF/PCM Solvation Model

	2	**3**	**4**	**5**	**6**	**7**	**8**	**9**	**10**
H(1)	0.6432	0.6402	0.6408	0.6414	0.6421	0.6414	0.6414	0.6424	0.6417
O(2)	−1.1104	−1.1399	−1.1389	−1.1396	−1.1397	−1.1401	−1.1381	−1.1389	−1.1387
C(3)	0.5915	0.6744	0.6753	0.6748	0.6733	0.6688	0.6769	0.6735	0.6745
C(4)	−0.0023	0.0165	0.0166	0.0160	0.0171	0.0186	0.0163	0.0176	0.0178
C(5)	0.0695	0.0434	0.0449	0.0449	0.0459	0.0460	0.0454	0.0472	0.0471
C(6)	0.8288	0.8460	0.8471	0.8459	0.8459	0.8449	0.8471	0.8472	0.8461
N(7)	−1.1783	−1.1951	−1.1949	−1.1945	−1.1945	−1.1945	−1.1924	−1.1935	−1.1928
C(8)	1.3965	1.3578	1.3565	1.3529	1.3545	1.3593	1.3572	1.3532	1.3570
O(9)	−1.1654	−1.1627	−1.1600	−1.1619	−1.1620	−1.1630	−1.1589	−1.1606	−1.1599
N(10)	−1.1333	−1.1441	−1.1456	−1.1420	−1.1416	−1.1444	−1.1404	−1.1398	−1.1392
H(11)	0.4193	0.4258	0.4358	0.4258	0.4258	0.4268	0.4277	0.4278	0.4285
C(12)	0.3557	0.3444	0.3734	0.3509	0.3515	0.3503	0.3586	0.3597	0.3639
C(13)	−0.0111	−0.0062	0.4363	0.0154	0.0148	−0.0147	0.0018	−0.0011	0.0295
C(14)	−0.0013	0.0169	0.0105	−0.0984	0.0383	−0.0029	0.0113	0.0008	−0.0664
C(15)	0.0127	−0.1132	−0.0128	0.0047	0.0048	−0.0023	−0.1697	−0.0013	0.4384
C(16)	−0.0034	0.0145	−0.0161	−0.0086	−0.0073	0.4445	0.0083	−0.1559	0.0203
C(17)	−0.0048	−0.0028	−0.0057	−0.0086	−0.0099	0.0128	0.0051	0.0087	0.0104

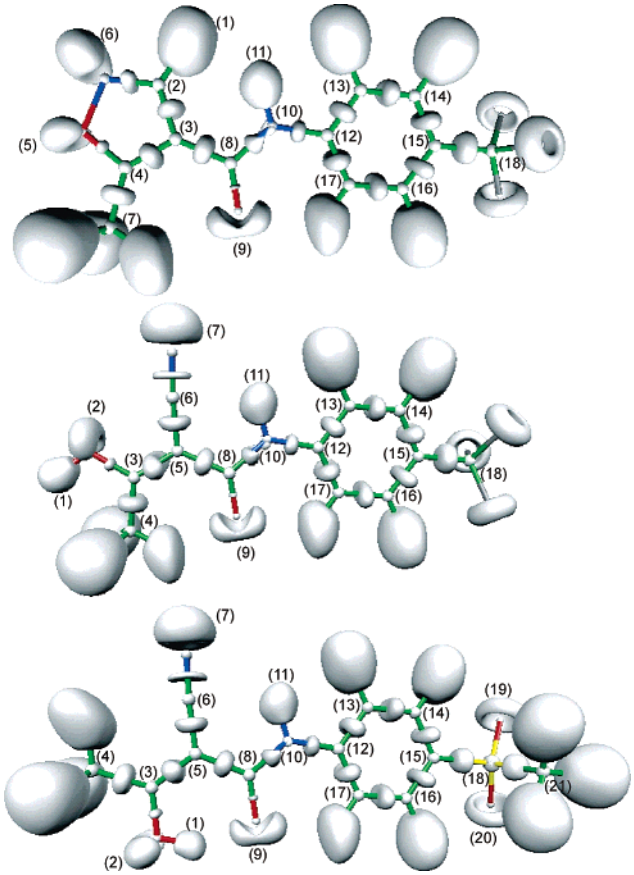

Figure 8. Electron localization function (ELF) isosurface of ELF = 0.85 for compounds **1** (top), **2** (middle), and **8** (bottom).

Table 7. Populations of ELF Basins for Leflunomide (Compound **1**)

basin type	gas-phase population	SCRF/PCM population
V(H1,C2)	2.18	2.19
V(H11,N10)	2.00	2.04
V(H13,C13)	2.14	2.15
V(H14,C14)	2.15	2.15
V(H16,C16)	2.14	2.15
V(H17,C17)	2.17	2.17
V(C3,C4)	3.39	3.37
V(C2,C3)	2.49	2.49
V(C3,C8)	2.35	2.35
V(C12,C13)	2.74	2.72
V(C13,C14)	2.91	2.89
V(C14,C15)	2.74	2.73
V(C15,C16)	2.87	2.88
V(C16,C17)	2.80	2.81
V(C17,C12)	2.80	2.79
V(C12,N10)	1.91	1.94
V(N10,C8)	2.15	2.23
V(N10)	1.67	1.52
V(C2,N6)	2.81	2.76
V(N6)	3.14	3.19
V(C8,O9)	2.25	2.21
V(O9)	5.45	5.50
V(C4,O5)	1.78	1.77
V(O5)	4.33	4.35
V(O5,N6)	1.10	1.09
V(C4,C7)	2.14	2.14

Comparison with Tables 4−6 shows that the ELF results provide additional chemical insight into a polar environment influence on the studied molecules. In all the compounds the SCRF/PCM model leads to an increase by 0.06 e in the population of the V(N7) basin, which is a nitrile nitrogen lone pair (for Leflunomide this is N6 atom of the isoxazole ring). This electron density is obtained by depletion of the V(C6,N7) bond. Similar changes are observed for the carbonyl group—V(O9) and V(C8,O9) basins. Note, however, that the V(N10,H11) fragment of the amide bond seems to be relatively unperturbed according to the ELF theory (with the exception of Leflunomide itself), while strengthening of the V(C8,N10) bond and depopulation of the V(N10) lone pair are clearly visible. It is also surprising that the basin populations of **2** are visibly different from those of **3**−**10** even for atoms located far from the O2−H1 group, the

Table 8. Populations of ELF Basins for Compounds **2**−**10** Calculated in the Gas Phase

basin type	**2**	**3**	**4**	**5**	**6**	**7**	**8**	**9**	**10**
V(H1,O2)	1.81	1.91	1.92	1.91	1.91	1.90	1.90	1.91	1.92
V(H11,N10)	2.02	2.02	2.03	2.03	2.03	2.03	2.03	2.03	2.03
V(H13,C13)	2.14	2.14		2.15	2.15	2.15	2.15	2.16	2.15
V(H14,C14)	2.15	2.16	2.14			2.15	2.15		
V(H15,C15)			2.15	2.16	2.16	2.15		2.18	
V(H16,C16)	2.15	2.15	2.15	2.14	2.14		2.15	2.14	2.14
V(H17,C17)	2.17	2.16	2.17	2.17	2.17	2.16	2.17	2.17	2.17
V(C3,C4)	2.13	2.10	2.10	2.11	2.11	2.11	2.11	2.12	2.10
V(C5,C3)	3.54	3.48	3.47	3.47	3.47	3.47	3.47	3.46	3.47
V(C5,C6)	2.35	2.40	2.40	2.40	2.40	2.41	2.40	2.40	2.41
V(C8,C5)	2.30	2.36	2.36	2.36	2.36	2.38	2.37	2.38	2.39
V(C12,C13)	2.74	2.78	2.93	2.81	2.82	2.77	2.74	2.79	2.84
V(C13,C14)	2.89	2.87	3.02	2.93	2.93	2.89	2.88	2.88	2.93
V(C14,C15)	2.77	2.83	2.76	2.82	2.84	2.78	2.79	2.81	2.96
V(C15,C16)	2.84	2.87	2.79	2.81	2.81	2.89	2.84	2.76	2.98
V(C16,C17)	2.81	2.82	2.80	2.80	2.79	2.95	2.81	2.79	2.81
V(C17,C12)	2.79	2.82	2.85	2.81	2.81	2.85	2.78	2.79	2.80
V(C12,N10)	1.93	1.91	1.92	1.92	1.92	1.92	1.93	1.93	1.93
V(N10,C8)	2.22	2.30	2.31	2.28	2.29	2.29	2.26	2.31	2.28
V(N10)	1.58	1.52	1.50	1.50	1.52	1.52	1.52	1.50	1.52
V(C6,N7)	4.40	4.35	4.36	4.34	4.36	4.35	4.35	4.36	4.35
V(N7)	3.25	3.29	3.28	3.29	3.29	3.30	3.29	3.28	3.29
V(C8,O9)	2.23	2.09	2.10	2.10	2.09	2.10	2.10	2.08	2.10
V(O9)	5.47	5.55	5.52	5.53	5.54	5.54	5.55	5.57	5.57
V(C3,O2)	1.61	1.71	1.70	1.70	1.71	1.70	1.72	1.71	1.71
V(O2)	4.27	4.09	4.10	4.11	4.11	4.09	4.10	4.11	4.09

Table 9. Populations of ELF Basins for Compounds **2**−**10** Calculated with SCRFPCM Solvation Model

basin type	**2**	**3**	**4**	**5**	**6**	**7**	**8**	**9**	**10**
V(H1,O2)	1.84	1.91	1.92	1.91	1.91	1.90	1.90	1.92	1.91
V(H11,N10)	2.03	2.04	2.04	2.04	2.04	2.04	2.04	2.04	2.04
V(H13,C13)	2.15	2.15		2.15	2.15	2.15	2.17	2.16	2.15
V(H14,C14)	2.15	2.16	2.15			2.15	2.15		
V(H15,C15)			2.16	2.16	2.16	2.16		2.17	
V(H16,C16)	2.15	2.15	2.15	2.15	2.15		2.15	2.15	2.14
V(H17,C17)	2.17	2.17	2.17	2.17	2.17	2.17	2.15	2.17	2.18
V(C3,C4)	2.13	2.10	2.11	2.11	2.11	2.11	2.12	2.11	2.11
V(C5,C3)	3.52	3.45	3.45	3.45	3.45	3.45	3.45	3.45	3.45
V(C5,C6)	2.38	2.43	2.42	2.43	2.42	2.43	2.42	2.42	2.42
V(C8,C5)	2.30	2.36	2.36	2.36	2.36	2.37	2.36	2.36	2.37
V(C12,C13)	2.73	2.77	2.92	2.80	2.81	2.76	2.73	2.80	2.82
V(C13,C14)	2.89	2.86	3.02	2.94	2.94	2.88	2.87	2.89	2.93
V(C14,C15)	2.76	2.83	2.75	2.82	2.83	2.77	2.79	2.80	2.96
V(C15,C16)	2.85	2.88	2.79	2.80	2.81	2.91	2.86	2.77	2.99
V(C16,C17)	2.82	2.82	2.80	2.80	2.80	2.95	2.82	2.78	2.82
V(C17,C12)	2.79	2.81	2.85	2.80	2.81	2.84	2.77	2.79	2.79
V(C12,N10)	1.94	1.93	1.93	1.93	1.92	1.93	1.94	1.92	1.93
V(N10,C8)	2.24	2.33	2.33	2.32	2.32	2.32	2.29	2.31	2.29
V(N10)	1.55	1.46	1.47	1.47	1.48	1.46	1.49	1.48	1.49
V(C6,N7)	4.34	4.28	4.30	4.28	4.30	4.29	4.29	4.30	4.30
V(N7)	3.31	3.35	3.34	3.35	3.35	3.35	3.35	3.35	3.35
V(C8,O9)	2.20	2.06	2.08	2.08	2.07	2.08	2.08	2.07	2.08
V(O9)	5.51	5.57	5.55	5.55	5.56	5.56	5.57	5.58	5.58
V(C3,O2)	1.62	1.71	1.71	1.72	1.72	1.71	1.73	1.72	1.72
V(O2)	4.22	4.10	4.10	4.11	4.12	4.10	4.11	4.10	4.11

position of which is the main difference between **2** and **3**−**10**. Let us return for a moment to Leflunomide (**1**) and Table 7. The weakest bond of the isoxazole ring is V(O5,N6) with a population of 1.1 e, smaller than for a formal single bond. This basin is, in comparison with the V(N6) population increase described above, only slightly influenced by the SCRF/PCM solvation model.

4. CONCLUSIONS

This work presents a comprehensive study of Leflunomide, its active metabolite, and the metabolite analogues using advanced methods of quantum chemistry. The geometry optimization in both gas-phase and solvent environments shows that the solvent influence on the structure is visible, but not great—in particular, the conformation is the same. The conformational part of our study has shown that planar arrangement of atoms is preferred for all the investigated compounds. For analogues **3**−**10** the intramolecular hydrogen bond is an important feature, which additionally stabilizes planar arrangement. The intramolecular proton transfer is energetically not preferred, but the barrier is lowered upon influence of the polar solvent reproduced by the SCRF/PCM model. Electron density and ESP differential maps showed the most sensitive places for external interactions in **1**−**10**. These places are located mostly around the N7, O9, and H11 atoms (in case of **1**: H1, O5, N6, O9, H11 atoms). These observations are fully supported by analysis of AIM atomic charges. The presence of an intramolecular hydrogen bond was confirmed theoretically by Popelier's criteria based on the AIM approach. The ELF method not only supports findings of electron density, ESP and AIM analyses, but also provides a chemical description of the electron density rearrangement in terms of uniquely defined localization domains (e.g. lone pairs or bonds). The electronic structure study presented here includes analysis of the polar environment influence. This analysis shows that the C≡N and amide groups of the compounds **2**−**10** are primary acceptors of the external interactions. The phenyl ring substituents play an important modifying role, but the electronic structure study shows that they act primarily on their own, not by changing the electron density distribution of the common part of the analogous compounds (atoms H1−H11).

ACKNOWLEDGMENT

The authors gratefully acknowledge the Wrocław Centre for Networking and Supercomputing (WCSS) and Academic Computer Center CYFRONET-KRAKÓW (Grants KBN/SGI/UWrocl/029/1998 and KBN/SGI/UWrocl/078/2001) for providing computer time and facilities.

REFERENCES AND NOTES

(1) Barinaga, M. From Bench Top to Bedside. *Science* **1997**, *278*, 1036−1039.
(2) Cherwinski, H. M.; Byars, N.; Ballaron, S. J.; Nakano, G. M.; Young, J. M.; Ransom, J. T. Leflunomide Interferes with Pyrimidine Nucleotide Biosynthesis. *Inflamm. Res.* **1995**, *44*, 317−322.
(3) Xu, X.; Shen, J.; Williams, J. W.; Gong, H.; Finnegan, A.; Chong, A. S−F. Two Activities of the Immunosuppressive Metabolite of Leflunomide, A77 1726. Inhibition of Pyrimidine Nucleotide Synthesis and Protein Tyrosine Phosphorylation. *Biochem. Pharm.* **1996**, *52*, 527−534.
(4) Fairbanks, I. D.; Bofill, M.; Ruckemann, K.; Simmonds, H. A. Importance of Ribonucleotide Availability to Proliferating T-lymphocytes from Healthy Humans. *J. Biol. Chem.* **1995**, *270*, 29682−29689.
(5) Xu, X.; Shen, J.; Mall, J. W.; Myers, J. A.; Huang, W.; Blinder, L.; Saclarides, T. J.; Williams, J. W.; Chong, A. S.-F. In vitro and in vivo Antitumor Activity of a Novel Immunomodulatory Drug, Leflunomide. Mechanisms of Action. *Biochem. Pharm.* **1999**, *58*, 1405−1413.
(6) Panico, A.; Cardile, V.; Gentile, B.; Garufi, F.; Fama, P.; Bonfiglio, G.; Ronsisvalle, G. Effects of Leflunomide on Human Cartilage. *Il Farmaco* **2003**, *58*, 983−987.
(7) Patterson, J. W.; Cheung, P. S.; Ernest, M. J. 3-Carboxy-5-methyl-N-[4-(trifluoromethyl) phenyl]-4-isoxazolecarboxamide, New Prodrug for the Antiarthritic Agent 2-cyano-3-hydroxy-N-[4-(trifluoromethyl)-phenyl]-2-butenamide. *J. Med. Chem.* **1992**, *35*, 507−510.
(8) Ghosh, S.; Zheng, Y.; Uckun, F. M. Five Analogues of the Active Metabolite of Leflunomide. *Acta Crystallogr.* **1999**, *C55*, 2117−2122.
(9) Ghosh, S.; Jennissen, J. D.; Zheng, Y.; Uckun, F. M. Three Leflunomide Metabolite Analogs. *Acta Crystallogr.* **2000**, *C56*, 1254−1257.
(10) Ghosh, S.; Narla, R.; Zheng, Y.; Liu, X.-P.; Jun, X.; Mao, C.; Sudbeck, E.; Uckun, F. M. Structure-based Design of Potent Inhibitors of EGF-receptor Tyrosine Kinase as Anti-Cancer Agents. *Anti-Cancer Drug Des.* **1999**, *14*(5), 403−410.
(11) Mahajan, S.; Ghosh, S.; Sudbeck, E. A.; Zheng, Y.; Downs, S.; Hupke, M.; Uckun, F. M. Rational Design and Synthesis of a Novel Anti-leukemic Agent Targeting Bruton's Tyrosine Kinase (BTK), LFM-A13 [α-Cyano-*β*-Hydroxy-*β*-Methyl-N-(2,5-Dibromophenyl) Propenamide]. *J. Biol. Chem.* **1999**, *274*(14), 9587−9599.
(12) Jöckel, J.; Wendt, B.; Löffler, M. Structural and Functional Comparison of Agents Interfering with Dihydroorotate, Succinate and NADH Oxidation of Rat Liver Mitochondria. *Biochem. Pharm.* **1998**, *56*(8), 1053−1060.
(13) Ren, S.; Wu, S. K.; Lien, E. J. Dihydroorotate Dehydrogenase Inhibitors: Quantitative Structure−Activity Relationship Analysis. *Pharm. Res.* **1998**, *15*(2), 286−295.
(14) Gaussian 03, Revision A.1, Frisch, M. J.; Trucks, G. W.; Schlegel, H. B.; Scuseria, G. E.; Robb, M. A.; Cheeseman, J. R.; Montgomery, J. A.; Vreven, T.; Kudin, K. N.; Burant, J. C.; Millam, J. M.; Iyengar, S. S.; Tomasi, J.; Barone, V.; Mennucci, B.; Cossi, M.; Scalmani, G.; Rega, N.; Petersson, G. A.; Nakatsuji, H.; Hada, M.; Ehara, M.; Toyota, K.; Fukuda, R.; Hasegawa, J.; Ishida, M.; Nakajima, T.; Honda, Y.; Kitao, O.; Nakai, H.; Klene, M.; Li, X.; Knox, J. E.; Hratchian, H. P.; Cross, J. B.; Adamo, C.; Jaramillo, J.; Gomperts, R.; Stratmann, R. E.; Yazyev, O.; Austin, A. J.; Cammi, R.; Pomelli, C.; Ochterski, J. W.; Ayala, P. Y.; Morokuma, K.; Voth, G. A.; Salvador, P.; Dannenberg, J. J.; Zakrzewski, V. G.; Dapprich, S.; Daniels, A. D.; Strain, M. C.; Farkas, O.; Malick, D. K.; Rabuck, A. D.; Raghavachari, K.; Foresman, J. B.; Ortiz, J. V.; Cui, Q.; Baboul, A. G.; Clifford, S.; Cioslowski, J.; Stefanov, B. B.; Liu, G.; Liashenko, A.; Piskorz, P.; Komaromi, I.; Martin, R. L.; Fox, D. J.; Keith, T.; Al-Laham, M. A.; Peng, C. Y.; Nanayakkara, A.; Challacombe, M.; Gill, P. M. W.; Johnson, B.; Chen, W.; Wong, M. W.; Gonzalez, C.; Pople, J. A. Gaussian, Inc., Pittsburgh, PA, 2003.
(15) Becke, A. D. Density-Functional Thermochemistry. III. The Role of Exact Exchange. *J. Chem. Phys.* **1993**, *98*, 5648−5652.
(16) Lee, C.; Yang, W.; Parr, R. G. Development of the Colle-Salvetti Correlation-Energy Formula into a Functional of the Electron Density. *Phys. Rev. B* **1988**, *37*, 785−789.
(17) Krishnan, R.; Binkley, J. S.; Seeger, R.; Pople, J. A. Self-consistent Molecular Orbital Methods. XX. A Basis Set for Correlated Wavefunctions. *J. Chem. Phys.* **1980**, *72*, 650−654.
(18) Frisch, M. J.; Pople, J. A.; Binkley, J. S. 25. Self-consistent Molecular Orbital Methods XXV. Supplementary Functions for Gaussian Basis Sets. *J. Chem. Phys.* **1984**, *80*, 3265−3269.
(19) Panek, J.; Stare, J.; Hadži, D. From the Isolated Molecule to Oligomers and the Crystal: A Static Density Functional Theory and Car-Parrinello Molecular Dynamics Study of Geometry and Potential Function Modifications of the Short Intramolecular Hydrogen Bond in Picolinic Acid N-Oxide. *J. Phys. Chem. A* **2004**, *108*, 7417−7423.
(20) Tomasi, J.; Persico, M. Molecular Interactions in Solution: An Overview of Methods Based on Continuous Distribution of the Solvent. *Chem. Rev.* **1994**, *94*, 2027−2094.
(21) Patrick, G. L. *An Introduction to Medicinal Chemistry*, 2nd ed.; Oxford University Press: Oxford, 2001.
(22) *3D QSAR in Drug Design. Theory, Methods and Applications*; Kubinyi, H., Ed.; ESCOM: Leiden, 1993.
(23) Bader, R. F. W.; Beddall, P. M. Virial Field Relationship for Molecular Charge Distributions and the Spatial Partitioning of Molecular Properties. *J. Chem. Phys.* **1972**, *56*, 3320−3329.
(24) Bader, R. F. W. *Atoms in Molecules, A Quantum Theory*; Clarendon Press: Oxford, 1990.
(25) Bader, R. F. W. AIMPAC, Suite of programs for the Theory of Atoms in Molecules; McMaster University, Hamilton, Ontario, Canada, 1991.
(26) Silvi, B.; Savin, A. Classification of Chemical Bonds Based on Topological Analysis of Electron Localization Function. *Nature* **1994**, *371*, 683−686.

(27) Noury, S.; Krokidis, X.; Fuster, F.; Silvi, B. Computational Tools for the Electron Localization Function Topological Analysis. *Comp&Chem.* **1999**, *23*, 597−604.
(28) Laaksonen, L. A Graphics Program for the Analysis and Display of Molecular Dynamics Trajectories. *J. Mol. Graph.* **1992**, *10*, 33−34.
(29) Portmann, S.; Lüthi, H. P. MOLEKEL: An Interactive Molecular Graphics Tool. *CHIMIA* **2000**, *54*, 766−770.
(30) Popelier, P. L. A. *Atoms in Molecules − An Introduction*; Pearson Education: Harlow, 2000.
(31) Jensen, F. *Introduction to Computational Chemistry*; Wiley-VCH: 1999.

CI049754D